

PROCEEDINGS OF SPIE

[SPIDigitalLibrary.org/conference-proceedings-of-spie](https://spiedigitallibrary.org/conference-proceedings-of-spie)

Wavefront coding with Jacobi-Fourier phase masks

E. González-Amador, A. Padilla-Vivanco, C. Toxqui-Quitl, M. Olvera-Angeles, J. Arines, et al.

E. González-Amador, A. Padilla-Vivanco, C. Toxqui-Quitl, M. Olvera-Angeles, J. Arines, E. Acosta, "Wavefront coding with Jacobi-Fourier phase masks," Proc. SPIE 11104, Current Developments in Lens Design and Optical Engineering XX, 1110405 (30 August 2019); doi: 10.1117/12.2523611

SPIE.

Event: SPIE Optical Engineering + Applications, 2019, San Diego, California, United States

Wavefront coding with Jacobi-Fourier phase masks

E. González-Amador^{*a,b}, A. Padilla-Vivanco^a, C. Toxqui-Quitl^a, M. Olvera-Angeles^{a,b}, J. Arines^c
and E. Acosta^b

^aUniversidad Politécnica de Tulancingo, Ingenierías No. 100, 43629, Hidalgo, Mexico.

^bDepartamento de Física Aplicada, Facultad de Óptica y Optometría, Universidad de Santiago de Compostela, 15782 Santiago de Compostela, A Coruña, Spain.

^cDepartamento de Física Aplicada, Facultad de Física, Universidad de Santiago de Compostela, 15782 Santiago de Compostela, A Coruña, Spain.

ABSTRACT

Wavefront coding is a hybrid optical-computational technique that makes use of a phase modulating element in conjunction with a deconvolution algorithm to extend the depth of focus of imaging systems. The phase mask codes the wave-front in such a way that the point-spread function do not change appreciably as a function of defocus. In this work, the modulation is introduced by phase masks in the shape of a subset of Jacobi-Fourier polynomials. We will show, by both numerical simulations and experiments that the Jacobi-Fourier polynomial phase masks are good candidates for high-resolution images under noise presence.

Keywords: Wavefront coding, Jacobi-Fourier, phase mask, trefoil phase mask, depth of focus, Gaussian noise, convolution-deconvolution.

1. INTRODUCTION

Wavefront coding (WFC) is a hybrid optical-computational technique that makes use of a phase modulating element in conjunction with a deconvolution algorithm to extend the depth of field or depth of focus (DOF) of a digital imaging system [1-2]. The trivial method for increasing DOF is to reduce the aperture of the instrument; in this way, the system presents less aberration, which results in better image quality. Nevertheless, a smaller aperture: 1) in-creases the role of diffraction, which limits the resolving power of optical instruments; and 2) reduces the amount of light that can be gathered by the system [3]. The other approach is to deconvolve the defocused images in order to deblur the out of focus regions. This approach has to main problems:

a) the response to the system (PSF) is not invariant under focus shifts and is therefore not known in most of the cases and,

b) deconvolution is an ill posed problem due to the loss of information for those special frequencies where the MTF is close or equal to zero. [4-5].

The technique known as WFC developed by Dowski and Cathey [1] proposes the simple placement of a phase mask (PM) at the exit pupil of the optical system that generates a controlled amount of third order aberrations. The aim of WFC is to modify the point spread function (PSF) in such a way that it becomes invariant over a range of distances around the image plane and MTF does not show zeroes. The coded images (intermediate images) look blurred and must be digitally filtered and an image close to diffraction-limited quality can be obtained [3].

From Dowski's proposal many shapes deriving from the original cubic phase mask solution have been proposed among them we can cite root square [4], trefoil [6], sinusoidal [7], free-form [8], among others. Recently, we have proposed a novel shape for the phase masks based on the Jacobi-Fourier polynomials [9]. These masks shape can be expressed as $r^{(p+1)/2} \cos(3\theta)$, where r denotes the radial coordinate, and the azimuthal dependence goes with $\cos(3\theta)$ same as trefoil mask. By changing the p value we obtain different shapes. We have shown by numerical simulations that the proper choice of the p value is a trade-off among signal to noise ratio, desired depth of focus and presence of artifacts. In this study, we study the performance of the masks by numerical and experimental analysis and compare with those for trefoil one which has been proven to perform better than cubic masks (less artifacts) [5,6].

This work is organized as follows: In section 2 we describe the Jacobi-Fourier phase masks (JFPM). In section 3 we analyze the optical properties of WFC system. Section 4 is devoted to show, analyze and discuss the numerical and experimental results. Lastly, in section 5 we present the conclusions.

* enrique.amador@upt.edu.mx phone (+52) 775 75 58 202

2. JACOBI-FOURIER PHASE MASK

Jacobi polynomials, $J_n(p, q, r)$, are a class of classic orthogonal polynomials in the interval $[0,1]$, where $n \geq 0$ indexes the set of orthogonal polynomials for given p and q values, and the independent variable r will represent in this work the radial coordinate normalized to the pupil radius. [10]

The Jacobi polynomials are chosen as the radial function for the phase masks and, hence, Jacobi-Fourier phase masks (JFPM) are defined as:

$$P_{nm}(p, q, r, \theta) = J_n(p, q, r) \cos(m\theta + \theta_0), \quad (1)$$

$J_n(p, q, r)$ denotes the Jacobi polynomials, and θ is the azimuthal angle. θ_0 denotes the angle of rotated JPPM and $m \geq 0$ the azimuthal frequency. We must stress the fact that not all combinations of m , p and q provide 2D polynomials separable in the x and y coordinates. Recently, it has been shown for cubic-like PM a smooth shape of the phase in the central part of the pupil and rapid variation at the periphery leads to non-zero and stable MTFs when defocusing [4]. In a recent work [9] we have shown that $p = q$ and $n = 0$ provide these feature and good coding performance can be obtained. Here, for the simulations and experimental demonstration we restrict ourselves to these values. For $m = 1$ JFPM extent the depth of focus in the same way as coma [11] but this is not as effective as trefoil, $m = 3$ [6, 12]. Moreover, when $p = 7$ and $m = 3$ the corresponding JFPM becomes trefoil aberration which has been shown to perform better than the pure cubic mask originally proposed by Dowski [1], and hence the results for the JFPM proposed here will be compared with those for trefoil one. Thus we will use

$$P_{0,3}(p, p, r, \theta) = J_0(p, p, r) \cos(3\theta + \theta_0), \quad (2)$$

3. OPTICAL PROPERTIES OF WFC SYSTEM WITH JFP PHASE MASK

For the numerical and experimental analysis, we considered an optical system consisting of a lens with a focal length of 100 mm and pupil diameter of 5 mm. The object is set at infinity illuminated with a monochromatic with a central wavelength of 632 nm. The JFPM is placed at the lens plane. We illustrate the results with the object at infinity for simplicity, but both the numerical and experimental analysis are also valid for any set of conjugated planes. For the numerical simulations the object and the PSF were convolved to simulate the intermediate image at high sampling rate, this image was then downsampled by factor to eight, resulting in $6.45\mu\text{m}$ pixels, to simulate the image captured by our experimental recording device. In order to analyze the performance of the mask in presence of noise we added random Gaussian noise to the intermediate coded images. Fourier transform of the intermediate image and Wiener filtering provide the final decoded images.

The generalized pupil function $\Pi_{n,p}(r, \theta)$ for the optical system can be expressed as:

$$\Pi_{n,p}(r, \theta) = \begin{cases} \exp[ik \phi_{n,p}(r, \theta)] & \text{if } r \leq 1 \\ 0 & \text{otherwise} \end{cases}, \quad (3)$$

where

$$\phi_{n,p}(r, \theta) = \alpha r^{\frac{p-1}{2}} \cos(3\theta - \pi/4) + W_{20} r^2, \quad (4)$$

α denotes the strength of the phase, $k = 2\pi/\lambda$ is the wave number, λ the wavelength, r the radius of the lens which has been normalized to unity and W_{20} represents the defocus

Figure 1 show the contour maps for $\alpha = 100\lambda$, we can observe, that the extension of the central plateau increases when the p value increases, and hence smaller PSFs.

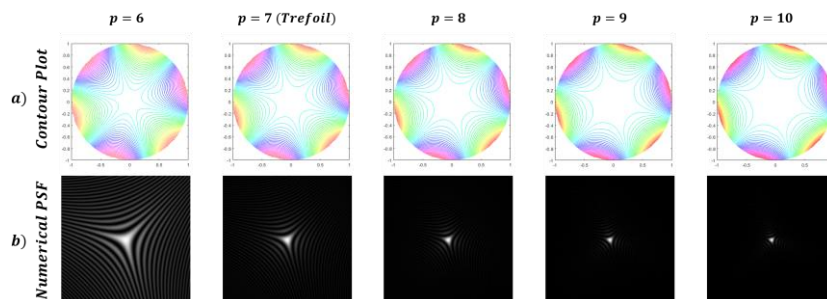


Figure 1. a) 2D contour maps for the phase mask, b) simulated PSF for JFPM and trefoil PM.

3.1 Analysis of optical properties of PM

In this section, we will analyze the modulation transfer functions (MTFs) and phase transfer function (PTFs) in X direction for the defocus interval [0,6mm] and two values of the strength, $\alpha = 7\lambda$ and $\alpha = 15\lambda$ (The choice of these values is constrained to our experimental device to mimic JFPM).

In figure 2 we plot the optical MTFs, denoted as $MTF(\alpha, W_{20})$,

Figure 3 show the PTFs of the system, $PTF_{System}(\alpha, W_{20})$, defined as:

$$PTF_{System}(\alpha, W_{20}) = PTF(\alpha, W_{20}) - PTF(\alpha, 0), \quad (5)$$

The figure show that for a given α , as p increases the amplitude of the $MTF(\alpha, W_{20})$ increases. On the other hand, as p increases there is a loss of invariance in the defocus range. All cases, the MTFs show ripples. Nevertheless, the number and height of oscillations decreases as p increases.

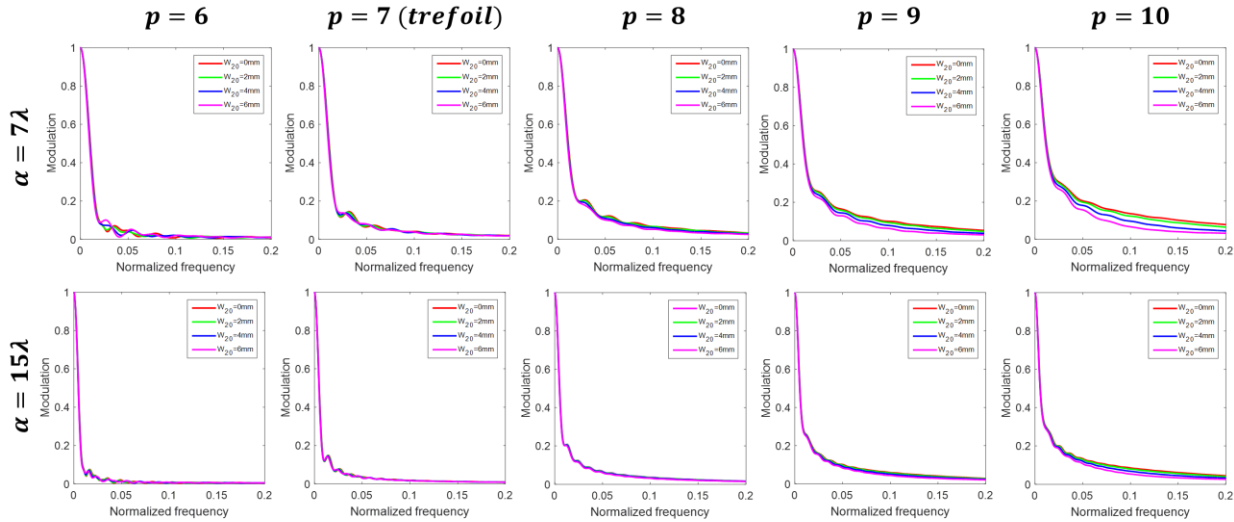


Figure 2. $MTF(\alpha, W_{20})$ corresponding to the different PM and defocus magnitudes for $\alpha=7\lambda$ and $\alpha=15\lambda$.

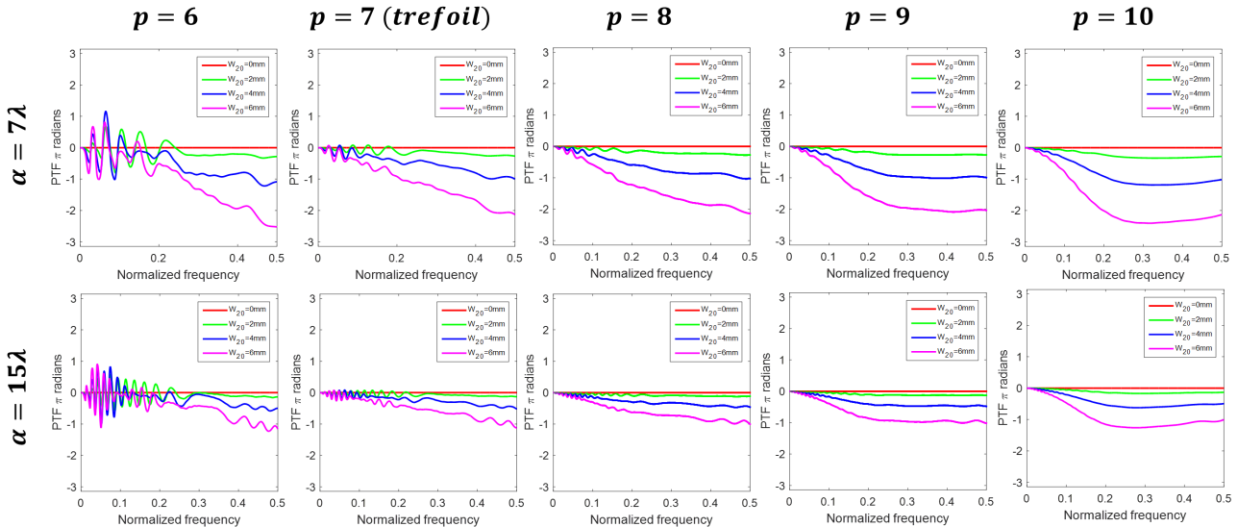


Figure 3. PTFs of system for $\alpha = 7\lambda$ and $\alpha = 15\lambda$

From figure 3, we can observe that for a given p and defocus value, as α increases the PTF becomes smaller. When $p = 6$ and $p = 7$ show an almost linear dependence between PTFs and frequencies. Nevertheless, when $p = 8$ relationship changes, where PTFs are steeper at small frequencies and change this behavior to become smooth functions that approach

asymptotically to a value. We can observe, that the value is closer to zero as p and α increases. Ripples can be show for small p values, in other hand, when value of p is bigger, the oscillations are smaller or null.

4. NUMERICAL AND EXPERIMENTAL RESULTS

In previous section we describe the optical properties of the different JFPM. In this section we will compare the simulated and experimental decoded images. We used a liquid crystal display (LCDs) as spatial light modulators to generate the phase masks in our WFC system (Holoeye®, model Pluto and a camera Hamamatsu ORCA-R2 C10600-10B). Such a display allows flexible implementation of different shape and strength PMs. Nevertheless, there are some limitations, for example, the maximum α value of the PM is limited 15λ . Therefore, the values we will use for the strength of the PMs are $\alpha = 7\lambda$ and $\alpha = 15\lambda$. Two different amounts of random Gaussian noise are added to the simulated intermediate images corresponding to a $CNR = 11.96$ (low level of noise) and $CNR = 4.84$ (high level noise). These values are obtained from the experimental intermediate images [13]. Figure 4 and figure 5 show the numerical and experimental results for $\alpha = 7\lambda$, $CNR = 11.96$ and $CNR = 4.84$ respectively. On the other hand, the results when $\alpha = 15\lambda$, correspond to the figure 6 and figure 7 for $CNR = 11.96$, and figure 8 for $CNR = 4.84$.

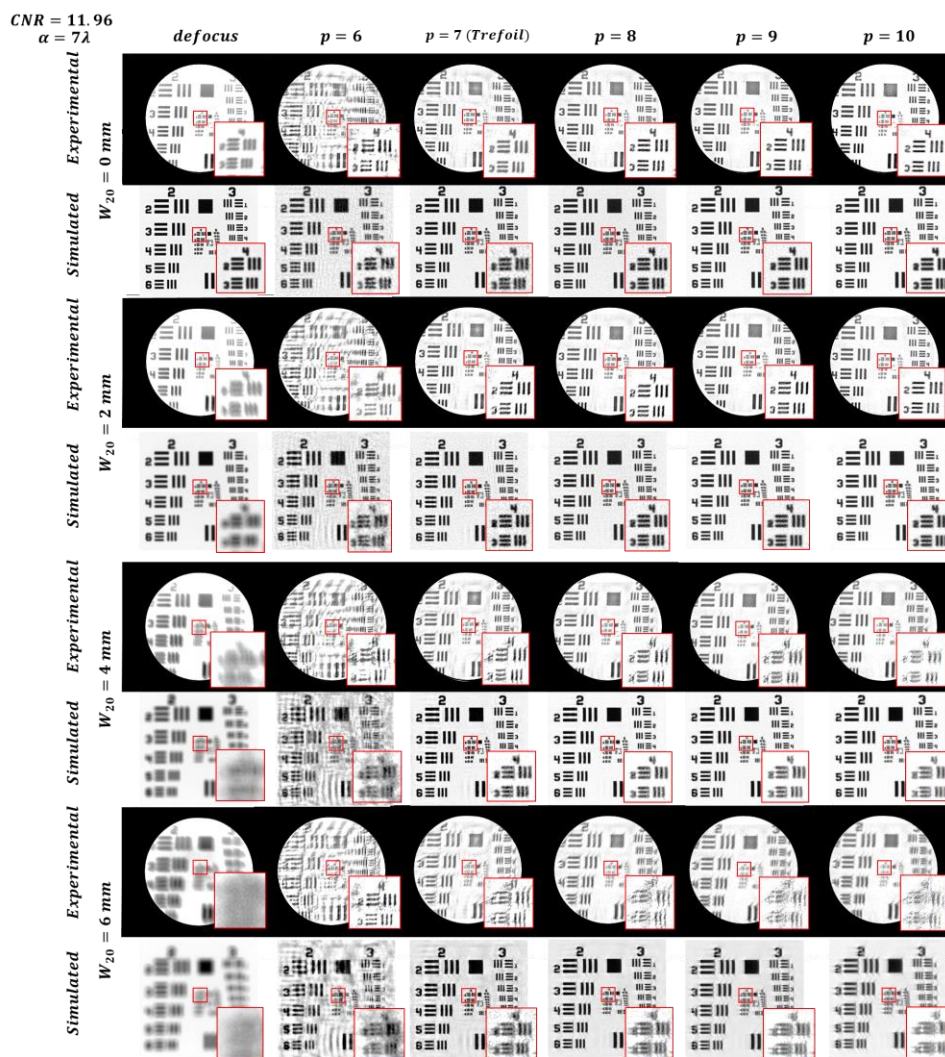


Figure 4. Experimental and corresponding simulated results for $\alpha = 7\lambda$ and $CNR = 11.96$.

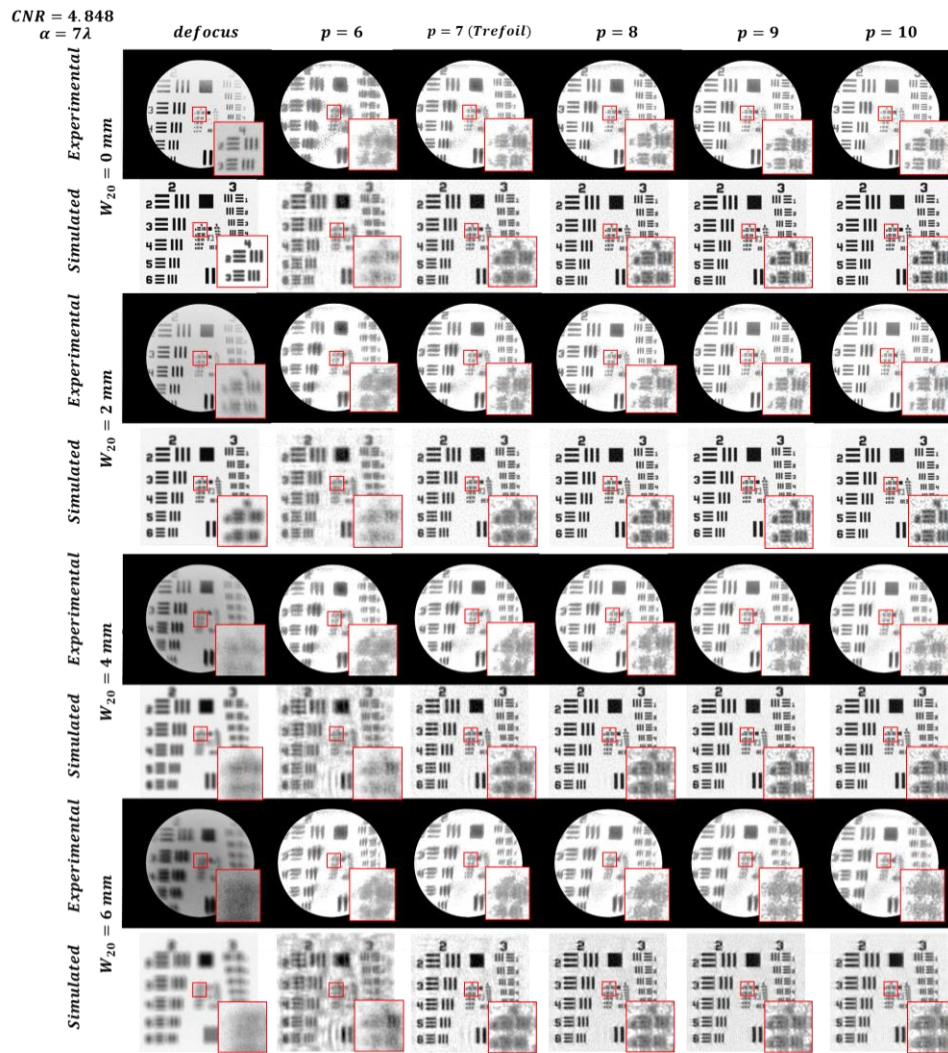


Figure 5. Experimental and corresponding simulated results for $\alpha = 7\lambda$ and $CNR = 4.848$.

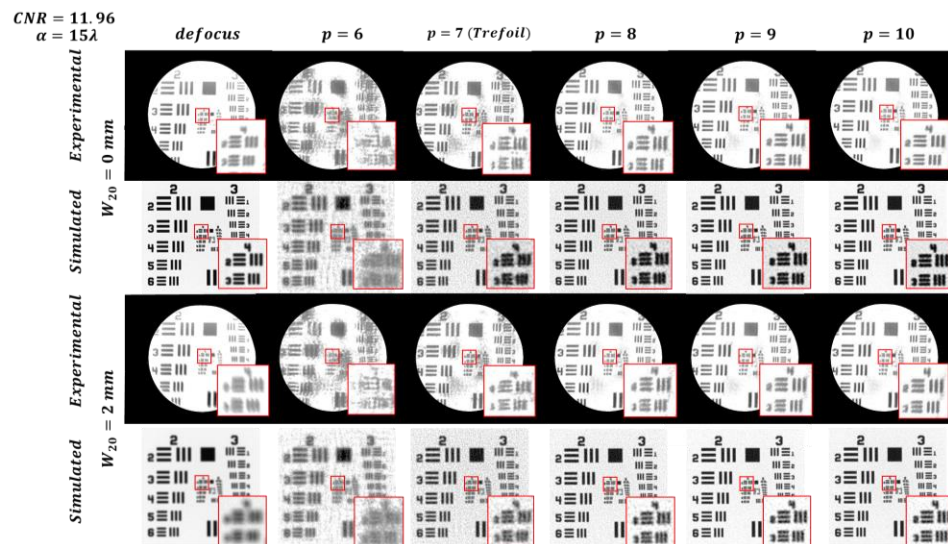


Figure 6. Experimental and corresponding simulated results for $\alpha = 15\lambda$ and $CNR = 11.96$.

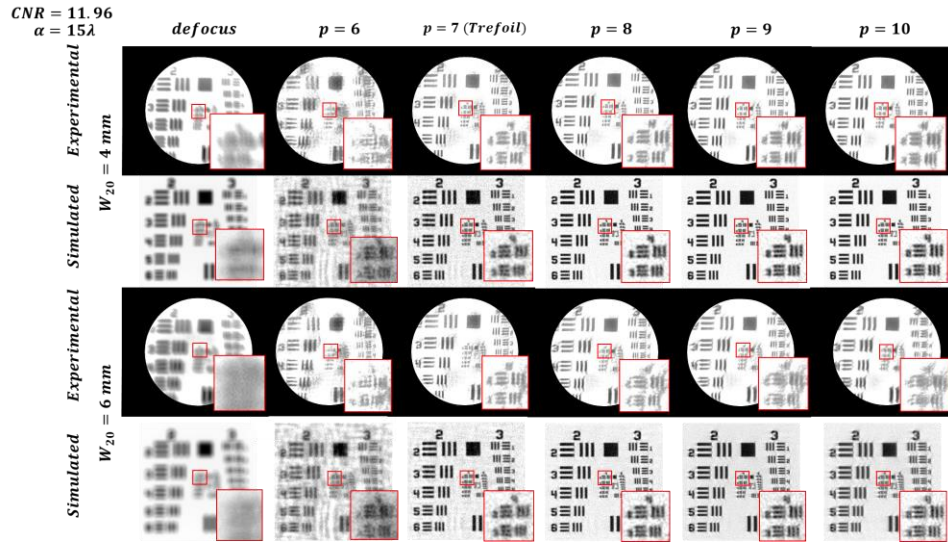


Figure 7. Experimental and corresponding simulated results for $\alpha = 15\lambda$ and $CNR = 11.96$. (Continuation of the figure 6)

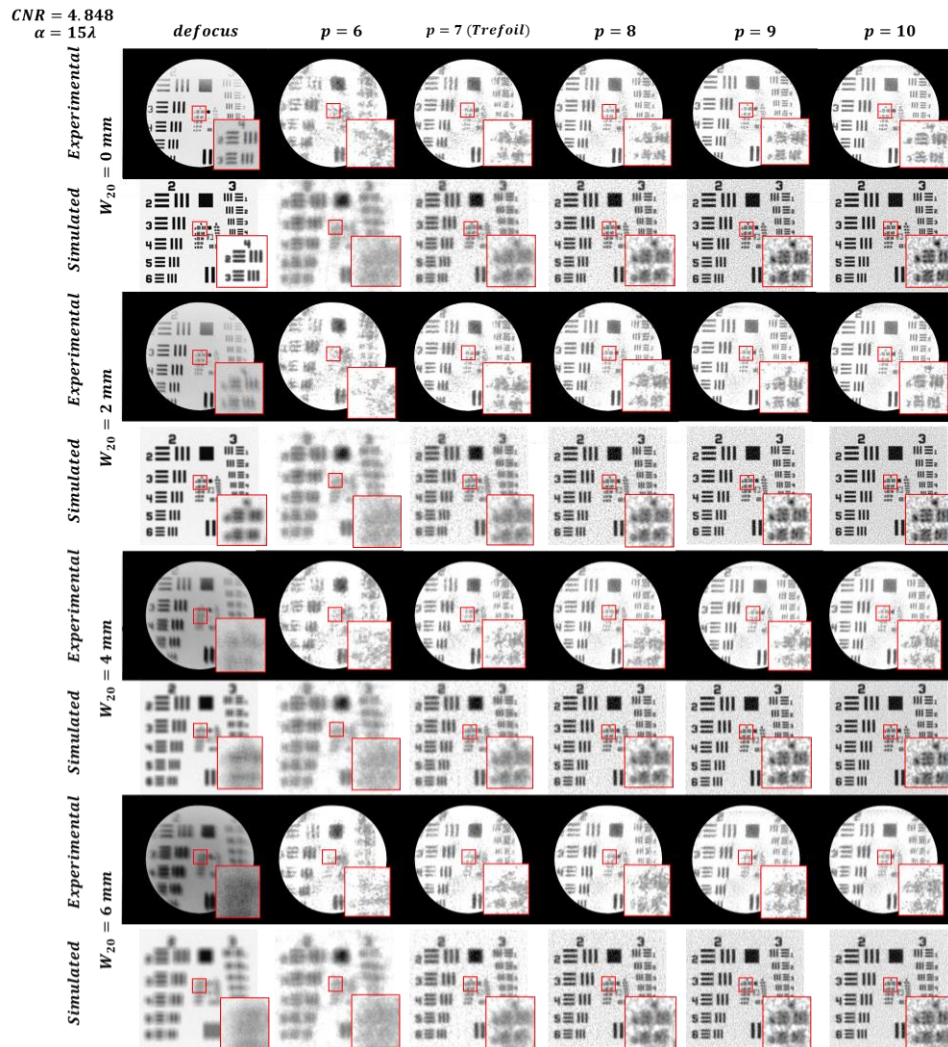


Figure 8. Experimental and corresponding simulated results for $\alpha = 15\lambda$ and $CNR = 4.848$.

4.1 Discussion

Simulated results agree with experimental ones. In all figures and in agreement with Demenikov et al [14] and Mo et al [15], we can assume that oscillations in the MTFs and related PTF's are the responsible of artifacts in the images. Artifacts due to oscillations in the high frequencies not noticeable because the MTFs are close to zero. For $p = 6$ and $p = 7$ show high oscillations in the MTFs for low frequencies whereas for higher values of p oscillations for low frequencies become very smooth or none and therefore artifacts are not noticeable. Invariance in the MTF's seems not to be important in what artifacts refer.

From the results, can be observed that grainy images are obtained. The amount of grain for a given level of noise decreases as p increases. More grain implies less details in images. Therefore, the range of defocus for small p values shrinks. The greater the value of α the grainier the images. All these results agree with the fact that the area under the $MTF(\alpha, W_{20})$ increases as p increases and/or α decreases. Noise softens artifacts but they are still visible for $p = 6$ and for $p=7$ and small defocus.

Therefore, from our point of view and for the optical system we have considered, the JFPM with $p = 8$ is the one that provides the best images for small level of noise and $\alpha = 7\lambda$ at expenses of shrink the defocus range; $p = 9$ provides the wider defocus interval and $p = 10$ the best images with an intermediate value of defocus range.

For high level of noise $p = 10$ provides the best results for both strength values but for $\alpha = 7\lambda$ the defocus range is slightly longer.

5. CONCLUSIONS

We use Jacobi-Fourier phase masks to extend the depth of focus in an optical imaging system. The radial part we used Jacobi polynomials, $J_{n,p}(\mathbf{r})$ with integer indexes. For the azimuthal dependence, we used $\cos(3\theta)$ in order to be able to draw comparisons with the well-known trefoil phase mask used for wavefront coding. In order to get a smooth central region in the masks, we used only $n = 0$ Jacobi polynomials. We found that values of p smaller than or equal to 7 yield decoded images with artifacts, the smaller the p value the higher the amount of artifacts.

For small values of p , the MTF curves have ripples which result in the presence of artifacts in the decoded images. Larger p value give rise to softer curves and hence fewer artifacts or none at all. The higher the p value the higher the MTF values and hence the best behavior in the presence of noise. However, invariance is gradually lost as p increases, which implies that as the value of p increases, depth of focus decreases. Results show that the Jacobi-Fourier phase masks are good candidates for WFC systems.

ACKNOWLEDGMENTS

This work was supported by the Spanish Ministry of Economía y Competitividad FIS2016-77319-C2-1-R, and FEDER, Xunta de Galicia/FEDER ED431B 2017/64 and ED431E 2018/08. E. González-Amador and M. Olvera-Angeles thank the Consejo Nacional de Ciencia y Tecnología (CONACYT); with CVU no 714742 and CVU no. 714741.

REFERENCES

- [1] Dowski, Edward R., and W. Thomas Cathey. "Extended depth of field through wave-front coding." *Applied optics* 34 (11), 1859-1866 (1995).
- [2] Dowski, Edward R., and Johnson, E. Gregory. "Wavefront coding: A modern method of achieving high performance and/or low cost imaging systems." In *Current Developments in Optical Design and Optical Engineering VIII*. Vol. 3779. International Society for Optics and Photonics, 137-146 (1999).
- [3] Ferran C, Bosch S, Carnicer A. "Design of optical systems with extended depth of field: an educational approach to wavefront coding techniques." *IEEE Transactions on Education*, 55(2), 271-278 (2012).
- [4] Nhu V, Fan Z, Minh NP, Chen S. "Optimized square-root phase mask to generate defocus-invariant modulation transfer function in hybrid imaging systems." *Optical Engineering*, 54(3), 035103 (2015).
- [5] Muyo G, Singh A, Andersson M, Huckridge D, Wood A, Harvey AR. "Infrared imaging with a wavefront-coded singlet lens." *Opt Express*, 17(23), 21118-21123 (2009).
- [6] Prasad S, Torgersen TC, Pauca VP, Plemmons RJ, van der Gracht J. "Engineering the pupil phase to improve image quality." In *Visual Information Processing XII*. Proc SPIE, 5108, 1-13 (2003).

- [7] Zhao H, Li Y. "Analytical and experimental demonstration of depth of field extension for incoherent imaging system with a standard sinusoidal phase mask." *Chinese Opt Lett*, 10(3), 031101 (2012).
- [8] Takahashi Y, Komatsu S. "Optimized free-form phase mask for extension of depth of field in wavefront-coded imaging." *Opt Lett*, 33(13), 1515-1517 (2008).
- [9] González-Amador, E. Padilla-Vivanco, A., Toxqui-Quitl, C., Arines, J., and Acosta, E. "Jacobi-Fourier polynomials phase mask for wavefront coding." *Optics and Lasers in Engineering*.
- [10] Bhatia AB, Wolf E. "On the circle polynomials of Zernike and related orthogonal sets". In *Mathematical Proc Cambridge Philosophical Society*, 50(1), 40-48 (1954).
- [11] Dorronsoro C, Guerrero-Colon JA, Marta C, Infante JM, Portilla J. "Low-cost wavefront coding using coma and a denoising-based deconvolution." In *Current Developments Electro-Optical and Infrared System Technology and Applications IV. Proc SPIE*, 6737:67370E (2007).
- [12] Kubala K, Dowski E, Cathey WT. "Reducing complexity in computational imaging systems." *Opt Express*, 11(18), 2102-2108 (2003).
- [13] Timischl, F. "The contrast-to-noise ratio for image quality evaluation in scanning electron microscopy." *Scanning*, 37(1), 54-62 (2015).
- [14] Demenikov M, Harvey A R. "Image artifacts in hybrid imaging systems with a cubic phase mask." *Optics express*, 18(8), 8207-8212 (2010).
- [15] Mo X, Wang J. "Phase transfer function based method to alleviate image artifacts in wavefront coding imaging system." In *International Symposium on Photoelectronic Detection and Imaging, Infrared Imaging and Applications. Proc SPIE*, 8907 89074H (2013).